CIRCUIT REALIZATION, ACTIVE BACK-STEPPING SYNCHRONIZATION OF SPROTT I SYSTEM AND APPLICATION TO SECURE COMMUNICATION

Supported by tetfund TERTIARY EDUCATION TRUST FUND

J. A. Laoye[1], A. D. Adelaja[1,2]* , T. O. Roy-Layinde[1] and R. K. Odunaike[1]
[1]Department of Physics, Olabisi Onabanjo University, Ago-Iwoye, Nigeria
[2]Department of Physics, Tai Solarin University of Education, Ijagun, Ijebu-Ode, Nigeria
*Corresponding author: ayodeleenochadelaja@gmail.com

Received: March 26, 2021 **Accepted:** June 18, 2021

Abstract: This study analyzed the Sprott I system through synchronization using active backstepping control, circuit realization and demonstrated its application to secure communication. The feasibility of the theoretical model of the Sprott I system was verified with the useful resource of the electronic circuit designed. Two identical Sprott I chaotic systems evolving from different initial conditions were globally synchronized by designing a nonlinear feedback controller using active backstepping technique. The controller was shown to effectively synchronize the Sprott I systems when activated. The application of the results to secure communication was presented numerically by synchronizing two chaotic Sprott I systems with a variable of the drive being encrypted information via a coupling channel. The encrypted signal was a superposition of sinusoidal information specified by a periodic function and chaotic carrier generated from a variable of the chaotic Sprott I system using additive encryption masking scheme. The transmitted information signal was shown to be retrievable from the chaotic response signal by inverse function decryption algorithm, thus confirming the effectiveness and robustness of the controller.

Keywords: Chaos, information, perturbation, encryption, simulation

Introduction

Edward Lorenz discovered inherent unpredictability (irregular motion with high sensitivity to initial conditions) and an associated structure called "butterfly effect" in a 3D weather model, and that was the first experimentally verified chaotic system (Lorenz, 1963). The butterfly effect is a manifestation of structure in chaos and it is a preliminary result in the studies of geometrical complexity known as fractal. This effect has made Lorenz system to serve as a prototype model for studying chaos for a long time. Due to diversity of complex systems in real-world applications, many other chaotic structures has been identified, this includes Rossler system (Rössler, 1976), Chen system (Chen & Ueta, 1999), Chua circuit (Tlelo-Cuautle & Duarte-Villaseñor, 2007), Sprott systems (Sprott, 1994), Sundarapandian systems (Sundarapandian & Pehlivan, 2012; Sundarapandian, 2013), Jerk system (Sambas *et al.*, 2015) and Financial systems (Cai & Huang, 2007; Yu-shu & Jun-hai 2001). Chaotic systems have several applications in the area of sciences, engineering, social sciences, chemical reactors, neural networks, robotics, information science, signal processing, financial economics, secure communication (Volos *et al.*, 2016; Vaidyanathan, 2015; Jafarov *et al.*, 2016; Yu *et al.*, 2016; Idowu *et al.*, 2018; Onma & Akinlami, 2017). In general, a nonlinear deterministic system with complex noise-like behavior characterized by limited predictability in the long time scale and high sensitivity to initial conditions is a chaotic system (Kurths *et al.*, 2003). This aperiodic behavior usually makes long-term predictions nearly impossible, and until recently, made chaotic systems undesirable, and the dynamics are to be eliminated in most practical applications. On the other hand, the ability of chaos to achieve a robust desired state through the amplification of small perturbation makes chaotic systems useful. Hence, the need for control through an established sequential structure that stabilizes targeted unstable periodic orbits to their equilibrium points through small time-dependent perturbations in any of the system's accessible variable or parameter, thereby improving the quality of the system behavior (Kurths *et al.*, 2003).

Controlled chaos and synchronization (forcing of two or more systems to cooperate with each other) of chaotic systems are generally advantageous and highly useful in many real-world applications including secure communication, earthquake dynamics, fluid mixing, time series analysis, heating and modeling brain and cardiac rhythm activities. The synchronization of chaos between master and slave chaotic systems which can simply be interpreted as transmitter and receiver relationship has been an area of recent research due to its potential applications in secure communication as an alternative to classical cryptography. Several control schemes have also been developed for the control of chaotic systems, such as active control (Sundarapandian, 2013), adaptive control (Lu & Cao, 2005; Onma*et al.*, 2016; Tirandaz & Hajipour, 2017), backstepping control (Vincent, 2008; Njah, 2010; Vincent *et al.*,2011), sliding mode control (Jang *et al.*, 2002; Nazzal & Natsheh, 2007; Vaidyanathan & Rhif, 2017), fuzzy control (Calvo& Cartwright, 1998; Hai-Peng, 2002), impulsive control (Chen*etal.*, 2004; Hua-Guang *et al.*, 2009), time-delay feedback (Park& Kwon, 2003), linear state error feed-back approach (Jiang, 2002) and finite-time control (Xiao-dong, 2009). Also, synchronization modes such as multiswitching combination synchronization, asymptotic synchronization, lag synchronization, cluster synchronization [(Hongmin & Qionghua, 2019) and references there in] have been adopted.

In practical applications, the design and implementation of chaos through simple physical systems such as electrical circuits has received a great deal of attention from scientists and engineers (Hongmin & Qionghua, 2019; Vaidyanathan, 2017), not only because of the potential positive implications of matching theories with experimental realizations, but also the possible real-world applications in diverse chaos-based advance technologies such as chaotic ratchets and memristors, and in information technologies. In view of the wide scope of possible applications of chaotic systems, this aspect remains an area of intensive research both to the theorists and control engineers. In a bid to generate chaotic systems that have real-world applications, Sprott embarked on a comprehensive quest to develop autonomous, 3D chaotic structures, however, among the many generated, only 19 cases (classified as 'A' to 'S') were found to be distinct(Sprott, 1994), and among this unique set only a few have electronic circuit design and potential practical applications. The control and synchronization of some of these Sprott systems has already been achieved, for instance, Vaidyanathan synchronized identical Sprott L and identical Sprott M systems, and non-identical Sprott L and M systems using active control (Vaidyanathan, 2012a) and adaptive control methods

(Vaidyanathan, 2012b). Synchronization based on other Sprott systems including Sprott E (Wang *et al.*, 2014), J (Islam *et al.*, 2015), K (Vaidyanathan , 2012c), A (Yılmaz & Ihsan, 2010; Melendez-Cano *et al.*, 2017), B (Melendez-Cano *et al.*, 2017), C (Melendez-Cano *et al.*, 2017), H (Cicek *et al.*, 2013; Melendez-Cano *et al.*, 2017), and R (Melendez-Cano *et al.*, 2017) has also been implemented. However, since no generalized results for the synchronization of chaotic systems of the same family (in this case the Sprott systems) has been achieved, it is necessary to consider new results for the synchronization of other Sprott systems that has not been implemented.

In this study, we realized the circuitry of Sprott I using OP-AMPS and appropriate circuit components in Multisim environment, and implemented it physically to observe the attractors on digital oscilloscope, designed an effective nonlinear controller $u_i(t)$which makes the state variables of the response (slave) system align (cooperate) with the variables of the drive (master) system, and stabilize the error vector of the state variables at the origin for all future state in finite time such that $\|e_i(t)\|_{\lim t\to\infty} = 0$ (its synchronization) via active backstepping scheme.

Model Description

The nonlinear system considered in this work is a Sprott chaotic system modeled as coupled first order ordinary differential equations of the form

$$\begin{aligned}\dot{x} &= -ay\\ \dot{y} &= x+z\\ \dot{z} &= x+y^2-z,\end{aligned} \qquad (1)$$

where the dot $|\cdot|$ denotes differentiation with respect to time. The SprottI system (Eqn. (1)) has a quadratic term and a positive real constant parameter a with x, y and z as the state variables. When $a = 0.2$, the system exhibits complex behavior with chaotic attractors depicted on a phase plot as shown in Fig. 1.

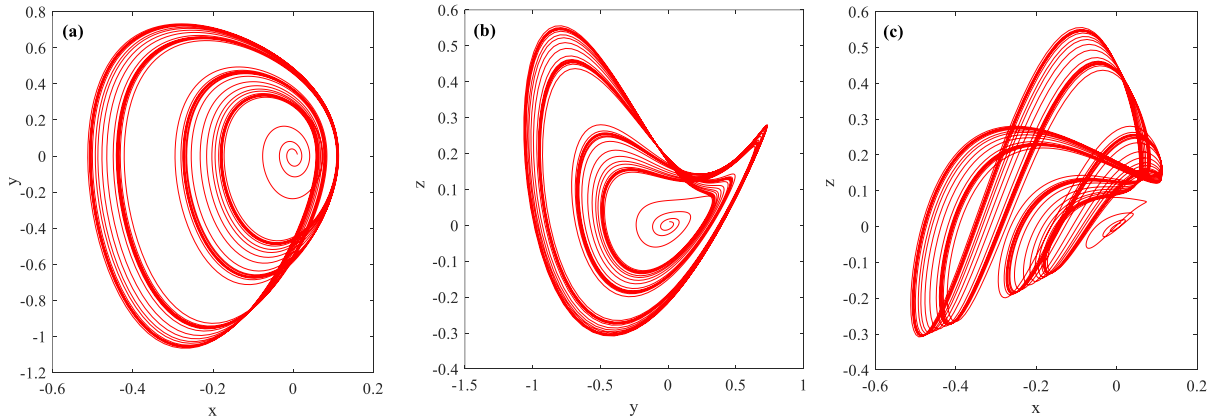

Fig. 1: Numerical results for the phase space attractors of Sprott I chaotic system with parameter $a = 0.2$, presented for (a) $x-y$ plane, (b) $y-z$ plane and (c) $x-z$ plane

The equilibrium of system (1) satisfies the following equations:

$$\begin{aligned}-ay &= 0\\ x+z &= 0\\ x+y^2-z &= 0.\end{aligned} \qquad (2)$$

Obviously, $E_0 = (0,0,0)$ is a unique equilibrium. For this reason, system (1) is linearized at equilibrium E_0 and the Jacobian matrix is given by:

$$\begin{bmatrix}0 & -a & 0\\ 1 & 0 & 1\\ 1 & 0 & -1\end{bmatrix}. \qquad (3)$$

The eigenvalues of equation (3) is obtained from $|\lambda I - J_0| = 0$, that is

$$\begin{bmatrix}-\lambda & -a & 0\\ 1 & -\lambda & 1\\ 1 & 0 & -(1+\lambda)\end{bmatrix} = 0. \qquad (4)$$

The Eigen values of the Jacobian matrix of system (1) at equilibrium point $E_0 = (0,0,0)$ are calculated as: $\lambda_1 = -1.13449,\ \lambda_{2,3} = 0.06725 \pm 0.58996i$.

This analysis is in agreement with already established description of the Sprott I system (Sundarapandian, 2012).

Electronic Circuit Implementation

In this section, we present the electronic circuit realization of Sprott I chaotic system (1) in order to view its attractors using MultiSIMvirtual electronic simulator and physically observe them on a digital oscilloscope from an assemblage of real electronic components. Each of the state variable x, y and z of system (1) is scaled to obtain suitable attractors within the dynamic range of operational amplifiers. An analogue circuitry designed in MultiSIM 14 software is displayed in Fig. 2a. The circuit consists of three channels which realize the integration addition and substation of the state variables x, y and z. The electronic circuit comprises electronic components such as resistors, capacitors and operational amplifiers, and an analog multiplier is used to execute the square function of the nonlinear term of the model. The multiplier operates over a dynamic range of ±1V with typical tolerance of less than 1%. The output signal (W) is connected

to those at inputs ($+X_1$), ($-X_2$), ($+Y1$), ($-Y2$), and ($+Z$) using the expression;
$W = \frac{(X_1 - X_2)(Y_1 - Y_2)}{10} + Z$. The circuital equation of the designed circuit shown in Figure 2 is obtained from Kirchhoff's laws, and it is given by;

$$dV_{C_1} = -\frac{1}{C_1 R_1} V_{C_2}$$

$$dV_{C_2} = \frac{1}{C_2 R_2}\frac{R_8}{R_7} V_{C_1} + \frac{1}{C_2 R_3}\frac{R_{10}}{R_9} V_{C_3} \qquad (5)$$

$$dV_{C_3} = \frac{1}{C_3 R_4}\frac{R_8}{R_7} V_{C_1} + \frac{1}{10}\frac{1}{C_3 R_5} V_{C_3},$$

where Vc_1, Vc_2 and Vc_3 are the voltages passing across the capacitors C_1, C_2 and C_3, respectively. The operational amplifiers used in the circuit are TL082CD and AD333JN was used as the multiplier of which the power supplies are $\pm 15 volts$. We set the values of the circuital components as follows: $C_1 = C_2 = C_3 = 10nF$, $R_1 = 50K\Omega$, $R_2 = R_3 = R_4 = R_6 = 10\ K\Omega$ and
$R_5 = R_7 = R_8 = R_9 = R_{10} = 1\ K\Omega$.

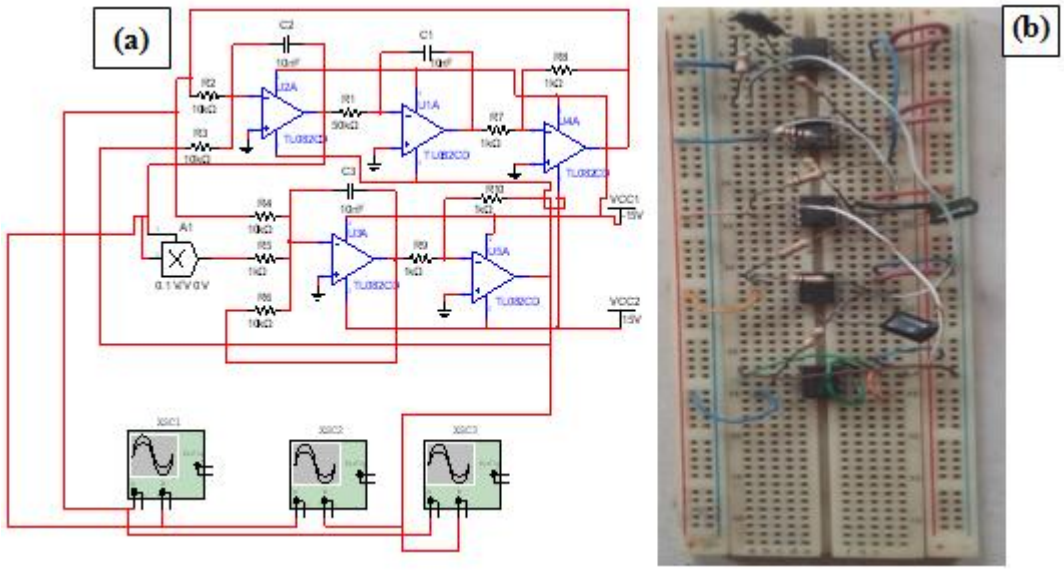

Fig. 2: (a) Schematic electronic circuit diagram of Sprott I chaotic system (b) Analog electronic hardware implementation of Sprott-I chaotic system

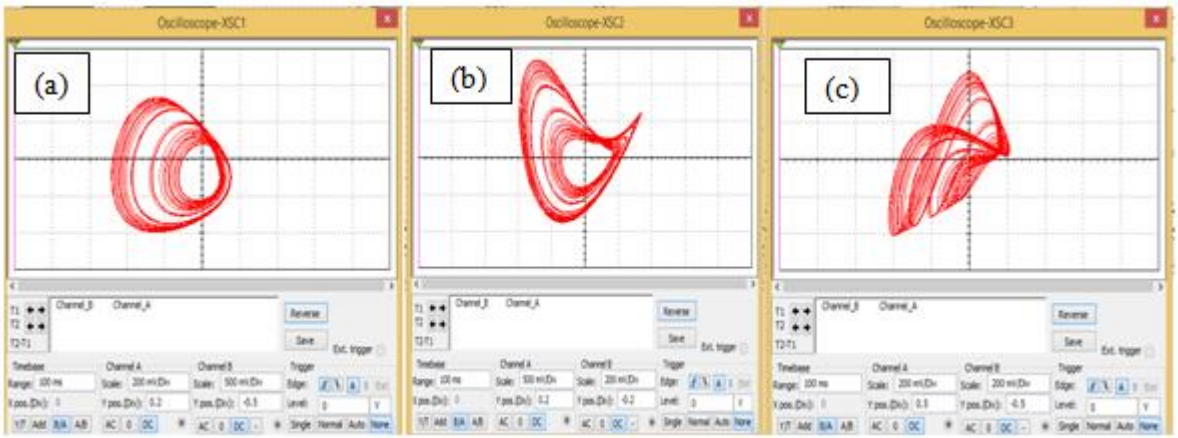

Fig. 3: The Phase space attractors of Sprott I chaotic system (1) as obtained from the oscilloscope of the MultiSIM circuit simulator for (a) $x - y$ plane (b) $y - z$ plane and (c) $x - z$ plane with capacitors $C_1 = C_2 = C_3 = 10nF$, resistors $R_1 = 50K\Omega$, $R_2 = R_3 = R_4 = R_6 = 10\ K\Omega$ and $R_5 = R_7 = R_8 = R_9 = R_{10} = 1\ K\Omega$

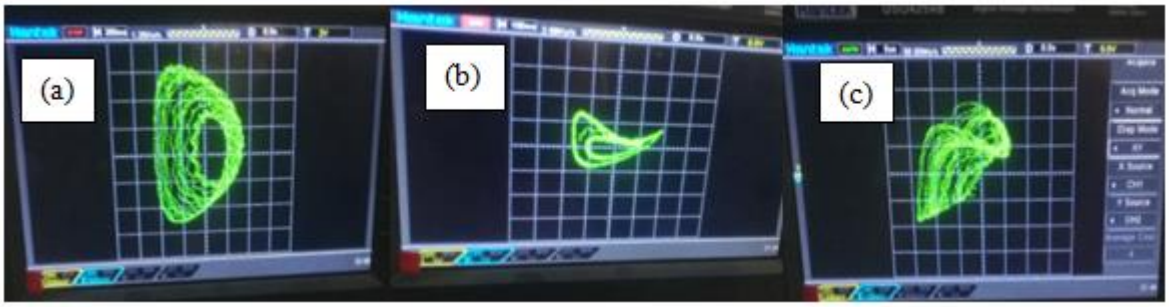

Fig. 4: The physical realization of the phase space attractors of Sprott I system (1) using off-the-shelf components as shown on the real oscilloscope (a) $x-y$ plane (b) $y-z$ plane and (c) $x-z$ plane with capacitors $C_1 = C_2 = C_3 =$ 10nF, resistors $R_1 = 50K\Omega$, $R_2 = R_3 = R_4 = R_6 = 10\ K\Omega$ and $R_5 = R_7 = R_8 = R_9 = R_{10} = 1\ K\Omega$

Using the circuit design approach based on operational amplifiers, the results presented in Fig. 3 display the various phase portraits of chaotic Sprott I system (1) when $a = 0.2$ as obtained in MultiSIM. It is obvious that the obtained oscilloscope results in Figures 3(a)--(c)are good realizations of the attractors presented for the numerical simulations shown in Figure 1(a)--(c), respectively and this confirms the feasibility of physically realizing the theoretical model using real electronic components. Having obtained promising results for both the numerical and the electronic simulations on MultiSIM, we afterwards, performed some laboratory experiments where the designed circuit in Fig. 2(a) was physically implemented on a breadboard (Fig. 2(b)). Fig. 4 depicts the oscilloscope results for the phase space attractors of the experimental realization. These results (Fig. 4(a-c) are in good agreement with the numerical and electronic simulations shown in Figures 1 and 3, respectively. With these results, we have physically implemented the Sprott I chaotic system. Next, we propose an active backstepping controller in other to synchronize two identical Sprott I systems with one being the drive (master) and the other is the response (slave).

Results and Discussion

Active backstepping synchronization for two identical chaotic sprott systems

To demonstrate the effectiveness of the active back-stepping synchronization scheme proposed herein, the control input is designed via active back-stepping technique to synchronize two identical Sprott chaotic systems:

First, we rewrite the system (Equation (1)) as

$$\begin{aligned} \dot{x}_1 &= -ax_2 \\ \dot{x}_2 &= x_1 + x_3 \\ \dot{x}_3 &= x_1 + x_2^2 - x_3. \end{aligned} \qquad (6)$$

Equation (6) is used as the drive or transmitter, and the response or receiver is given by

$$\begin{aligned} \dot{y}_1 &= -ay_2 + u_1(t) \\ \dot{y}_2 &= y_1 + y_3 + u_2(t) \\ \dot{y}_3 &= y_1 + y_2^2 - y_3 + u_3(t), \end{aligned} \qquad (7)$$

Where the control inputs are represented as $u_1(t), u_2(t), u_3(t)$. The synchronization error vector is obtained by subtracting equation (7) from equation (6), and using the usual notation $e_i = y_i - x_i$, it is given by

$$\begin{aligned} \dot{e}_1 &= -e_2 + u_1 \\ \dot{e}_2 &= e_1 + e_3 + u_2 \\ \dot{e}_3 &= 2x_2e_2 + e_1 + e_2^2 - e_3 + u_3. \end{aligned} \qquad (8)$$

The first equation in equation (8) is stabilized by regarding e_2 as a virtual controller. By selecting the Lyapunov function $V_1(e_1) = \frac{1}{2}e_1^2$ and differentiating it along the trajectory of time, we obtain

$$\dot{V}_1(e_1) = e_1\dot{e}_1 = e_1[-ae_2 + u_1]. \qquad (9)$$

The controller e_2 is estimated as $e_2 = \alpha_1(e_1)$, hence equation (9) becomes $\dot{V}_1(e_1) = e_1[-a\alpha_1(e_1) + u_1]$. With the choice of $\alpha_1(e_1) = e_1$ and $u_1 = 0$, $\dot{V}_1 = -ae_1^2$ (negative definite).

The error ω_2 between e_2 and $\alpha_1(e_1)$ is defined as:

$$\omega_2 = e_2 - \alpha_1(e_1) = e_2 - e_1 \qquad (10)$$

Substituting $\dot{e}_2$, $\dot{e}_1$ and e_2 from equations (8) and (9), respectively into the time derivative of equation (10) yields

$$\dot{\omega}_2 = e_1 + e_3 + a(\omega_2 + e_1) + u_2. \qquad (11)$$

The subsystem (e_1, ω_2) given by equation (11) is stabilized as follows: By regarding the Lyapunov function V_2 as; $V_2(e_1, \omega_2) = \dot{v}_1(e_1) + \frac{1}{2}\omega_2^2$ of which the time derivative is given in equation (12).

$$\dot{V}_2(e_1, \omega_2) = \dot{v}_1(e_1) + \omega_2\dot{\omega}_2 \qquad (12)$$

From equations (9) and (10),

$$\dot{v}_1 = -ae_1^2 - ae_1\omega_2. \quad (13)$$

Hence,

$$\dot{V}_2(e_1,\omega_2) = -ae_1^2 + \omega_2[e_1 + e_3 + a(\omega_2 + e_1) + u_2] \quad (14)$$

If e_3 is measurable and estimated as $e_3 = \alpha_2(e_1,\omega_2)$, the equation (12) becomes;

$\dot{V}_2(e_1,\omega_2) = -ae_1^2 + \omega_2[e_1 + \alpha_2(e_1,\omega_2) + a(\omega_2 + e_1) + u_2]$.

If $\alpha_2(e_1,\omega_2) = 0$ and $u_2 = -(e_1 + 2a\omega_2)$, then $\dot{V}_2 = -ae_1^2 - a\omega_2^2$ (negative definite, since $a > 0$).

Finally, the complete system (e_1,ω_2,ω_3) is stabilize by regarding error between e_3 and $\alpha_2(e_1,\omega_2)$ as ω_3.

$$\omega_3 = e_3 - \alpha_2(e_1,\omega_2) = e_3. \quad (15)$$

The substitution of $\dot{e}_3$, e_3 and e_2 from equations (8), (15) and (10), respectively into the time derivative of equation (15) gives

$$\dot{\omega}_3 = e_1 + 2x_2(\omega_2 + e_1) + (\omega_2 + e_1)^2 - \omega_3 + u_3 \quad (16)$$

The Lyapunov function V_3 is defined as $V_3(e_1,\omega_2,\omega_3) = v_2(e_1,\omega_2) + \frac{1}{2}\omega_3^2$, and its time derivative is given by; $\dot{V}_3(e_1,\omega_2,\omega_3) = \dot{v}_2 + \omega_3\dot{\omega}_3$.

Hence,

$$\dot{V}_3(e_1,\omega_2,\omega_3) = -ae_1^2 - a\omega_2^2 + \omega_3[e_1 + 2x_2(\omega_2 + e_1) + (\omega_2 + e_1)^2] - \omega_3 + u_3. \quad (17)$$

If $u_3 = -[e_1 + 2x_2(\omega_2 + e_1) + (\omega_2 + e_1^2)^2]$, then equation (17) reduces to;

$\dot{V}_3(e_1,\omega_2,\omega_3) = -ae_1^2 - a\omega_2^2 - \omega_3^2$ (negative definite). Therefore, the control units necessary for the synchronization of the identical Sprott I systems are given by

$$\begin{aligned} u_1 &= 0 \\ u_2 &= -(e_1 + 2a\omega_2) \quad (18) \\ u_3 &= -[e_1 + 2x_2(\omega_2 + e_1) + (\omega_2 + e_1)^2], \end{aligned}$$

and the synchronization norm e can be computed by

$$e = \sqrt{e_1^2 + e_2^2 + e_3^2}. \quad (19)$$

The classical Fourth-Order Runge-Kutta routine was used to solve systems (6) and (7) with the control inputs as defined by equation (18) using the initial conditions of the drive (equation (6)) and response (equation (7)) systems as: $(x_1, x_2, x_3) = (0.01, -0.02, 0.01)$ and $(y_1, y_2, y_3) = (0.03, 0.01, -0.09)$, respectively, with a time step of 0.001. To ensure all the state variable of the two systems undergo chaotic dynamics, the value of the real positive constant parameter a is fixed as $a = 0.2$. The simulation results for the synchronization of two Sprott I systems (Equations (6) and (7))are presented in Figures 5 and 6. Fig. 5(a-c) shows the state trajectories of the drive (Equation (6)) and the response (Equation(7)) systems with different initial conditions, with continuous red and green lines indicating the trajectories of the drive and the response variables, respectively. Fig. 5 shows that the systems are in unsynchronized states from the unset of their dynamics, but immediately the controller was activated at $t = 500$ the trajectory of the response tracks with that of the drive and as such both trajectories became perfectly superposed on each other at a time $t \geq 500$ giving a false indication that the trajectories collapsed into a single trajectory (which is that of the drive)for a pair of comparable system variables $(x_1, y_1), (x_2, y_2)$ and (x_3, y_3) shown in Fig. 5 (a), (b) and (c), respectively. This clearly means the systems were in unsynchronized state within $0 \leq t \leq 500$, and in synchronous state within $500 < t \leq 1000$.

The error dynamics between the drive and the response system (obtained from equation (8)) before and after the controller was switched on is shown in Fig. 6. The error vector shows chaotic dynamics with time when the controller is not activated, and when the controller is switched on at $t = 500$ the error vector converge to equilibrium point as shown in Figure 6(a)-(c), thereby guaranteeing the synchronization of systems (6) and (7).The time evolution of the synchronization norm (equation (19)) validates that the two chaotic systems became synchronized when the controller was switched on as presented in Fig. 6(d).

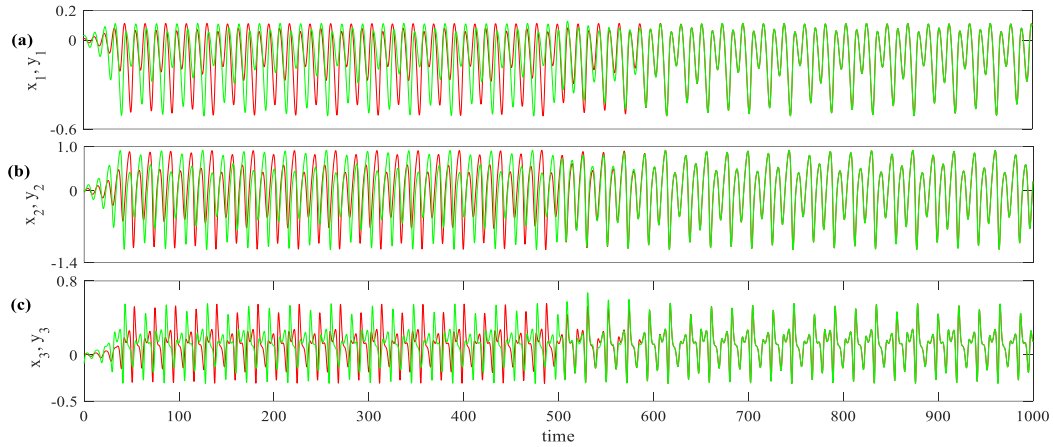

Fig. 5: The time response of the state variables (x_1, x_2, x_3) of the drive system (Equation (6)) with continuous green lines and the corresponding state variables (y_1, y_2, y_3) of the response system (Equation (7))with continuous red lines showing the controller was activated at $t = 500$ for (a) (x_1, y_1), (b) (x_2, y_2) and (c) (x_3, y_3)

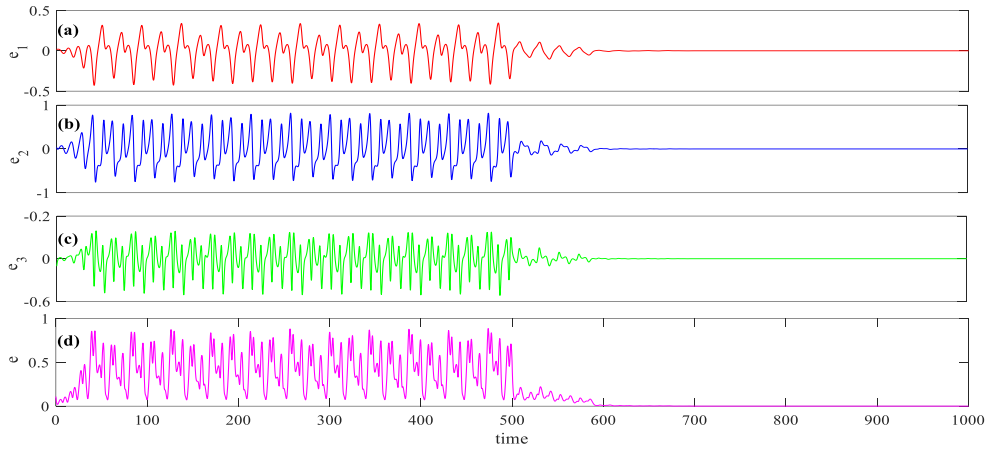

Fig. 6: Error dynamics between the variables (x_1, x_2, x_3) of the drive system (6) and their corresponding variables (y_1, y_2, y_3) of the response system (7) showing the controller was switched on at $t = 500$ for (a) $e_1 = y_1 - x_1$, (b) $e_2 = y_2 - x_2$, (c) $e_3 = y_3 - x_3$ and (d) the synchronization norm e using Equation (19)

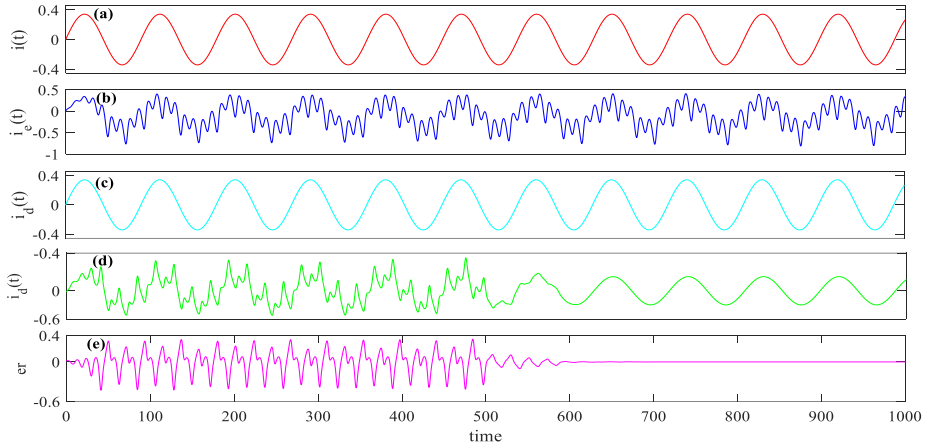

Fig. 7: Sprott I system masking communication; (a) input/information signal $i(t)$, (b) encrypted signal $i_e(t)$ and (c) output/decrypted signal $i_d(t)$ (d) the decrypted signal $i_d(t)$ activated at time $t = 500$ and, (e) decryption error er corresponding to Figure 7(d)

Chaotic masking application to secure communication

The sensitivity to initial conditions and randomness which are associated with chaos can be leveraged upon in engineering applications, particularly in the field of secure communication where information is being protected by embedding it in chaotic signals during transmission. Synchronization and encryption are major processes that are necessary for implementation of chaotic secure communication. To achieve encryption with chaotic signals, information signals are mixed with chaotic carrier signals through mixing algorithm known as chaotic masking scheme. Many mixing algorithms such as additive masking and multiplicative masking had been used in order to achieve chaotic masking (Onma& Akinlami, 2017; Onma *et al*., 2017; Busawon *et al.*, 2018; Hreshee *et al.*, 2018; Adel Ouannas, 2021).

In this work, additive encryption masking scheme is employed to demonstrate the application of chaos to secure communication. The information signal (input) used is a periodic function of the form $i(t) = 0.3\sin 0.07t$ and the chaotic carrier chosen is the drive variable x_1 of the Sprott I system given by Equation (6). The masking algorithm $i_e(t) = i(t) + x_1$ gives the encrypted information $i_e(t)$ which is used in place of variable x_1 of the drive system, so that the information signal is masked in the encrypted information at a variable of the transmitter. Conversely, to retrieve the information at the receiver (output), the decrypted information $i_d(t)$ is obtained from the inverse function $i_d(t) = i_e(t) - y_1$, where y_1 is a variable of the response system (see Equation (7)) corresponding to the location of the encrypted signal in the drive. Here, the drive is regarded as the transmitter while the response is the receiver. Transmission of information from the transmitter to the receiver is achieved viathe synchronization of the drive system which contains the encrypted information and the response system via a coupling channel. The coupling channel used is our designed active backstepping controller, and the effectiveness of the communication scheme is shown in Fig. 7. Fig. 7(a–c) shows the sinusoidal wave form of the periodic information signal $i(t)$, the encrypted chaotic masking signal $i_e(t)$ which is being transmitted and the retrieved signal (decrypted signal) $i_d(t)$, respectively. For a clearer picture of the process, the inverse function for the decrypted signal is activated at time $t = 500$, and the corresponding decryption error is computed from $er = i(t) - i_e(t)$.

Clearly, it can be observed from Figure 7(d) that the information signal is masked in chaotic signal between $0 \le t \le 500$ before we initiated decryption process, and the decrypted signal at $t > 500$ is the transmitted sinusoidal information. Also, the decryption error presented in Fig. 7(e) shows the error dynamics approaches zero immediately the decryption function was activated (at $t = 500$), and it eventually settled at zero confirming the chaos dies out at $t > 500$, and the retrieved output information is the multistable periodic function (the input). Finally, the encrypted chaotic information can be decrypted to retrieve the input information at any time and the dynamics of the decrypted error validates the usefulness of this process in secure information.

Conclusion

In this work, we have analyzed the Sprott I chaotic circuit using numerical simulation, and achieved circuit realization using electronic circuit simulator (MultiSIM) as well as physical implementation with real electronic components connected to an oscilloscope. The oscilloscope results of the attractors from the designed circuit were in agreement with simulations from the mathematical model. Active backstepping technique was applied to synchronize two identical chaotic Sprott I systems evolving from differential initial conditions. The designed controller robustly synchronized the two Sprott I systems. The synchronization results were extended to secure communication and we explained the possibility of applying the results to secure information using additive encryption masking scheme with chaotic wave form x_1 as carrier and $i(t)$ as the information signal. The numerical simulations demonstrated the validity and effectiveness of the proposed controller. Hence, these results can be applied in practical applications such as cryptosystem, encryption, neural networks and secure communication.

Conflict of Interest

The authors declare that there is no conflict of interest related to this work.

References

Cai G & Huang J 2007. A new finance chaotic attractor. *Int. J. Nonlinear Sci.*, 3(3): 213-220.

Calvo O & Cartwright JH 1998. Fuzzy control of chaos. *Int. J. Bifurcation and Chaos*, 8(8): 1743-1747.

Chen G & Ueta T 1999. Yet another chaotic attractor. *Int. J. Bifurcation and Chaos*, 9(7): 1465-1466.

Chen S, Yang Q & Wang C 2004. Impulsive control and synchronization of unified chaotic system. *Chaos, Solitons & Fractals*, 20(4), 751-758.

Cicek S, Uyaroğlu Y & Pehlivan I 2013. Simulation and circuit implementation of sprott case H chaotic system and its synchronization application for secure communication systems. *J. Circuits, Sys. and Comp.*, 22(4): 1350022.

Hai-Peng R & Ding L 2002. Chaos control and anti-control via a fuzzy neural network inverse system method. *Chinese Physics Letters*, 19(8): 1054.

Hongmin D & Qionghua W 2019. The Synchronisationof two floating memristor-basedoscillators and the circuit design. *Pramana*, 93: 49.

Hua-Guang Z, Tie-Dong M, Jie F & Shao-Cheng T 2009. Robust lag synchronization between two different chaotic systems via dual-stage impulsive control. *Chinese Physics B*, 18(9): 3751.

Idowu BA, Vaidyanathan S, Sambas A, Olusola OI & Onma OS 2018. A new chaotic finance system: Its analysis, control, synchronization and circuit design. In *Nonlinear Dynamical Systems with Self-Excited and Hidden Attractors* (pp. 271-295). Springer, Cham.

Islam M, Islam N & Nikolov S 2015. Adaptive control and synchronization of Sprott J system with estimation of fully unknown parameters. *J. Theoretical and Appl. Mechan.*, 45(2): 45-58.

Jafarov SM, Zeynalov ER & Mustafayeva AM 2016. Synthesis of the optimal fuzzy TS controller for the mobile robot using the chaos theory. *Procedia Computer Science*, 102: 302-308.

Jang MJ, Chen CL & Chen CO 2002. Sliding mode control of chaos in the cubic Chua's circuit system. *Int. J. Bifurcation and Chaos*, 12(6): 1437-1449.

Jiang ZP 2002. Advanced feedback control of the chaotic Duffing equation. *IEEE Transactions on Circuits and*

Systems I: Fundamental Theory and Applications, 49(2): 244-249.

Kurths J, Boccaletti S, Grebogi C & Lai YC 2003. Introduction: Control and synchronization in chaotic dynamical systems. *Chaos: An Interdisc. J. Nonlinear Sci.,* 13(1): 126.

Lorenz EN 1963. Deterministic Nonperiodic Flow. In *The Theory of Chaotic Attractors* (pp. 25-36). New York, NY.: Springer.

Lu J & Cao J 2005. Adaptive complete synchronization of two identical or different chaotic (hyperchaotic) systems with fully unknown parameters. *Chaos: An Interdisc. J. Nonlinear Sci.,* 15(4): 043901.

Melendez-Cano A, Rodriguez JS, Sandoval-Ibarra Y, Cardenas-Valdez JR, Garcia-Ortega MJ, Tlelo-Cuautle E et al. 2017. Chaotic Synchronization of Sprott Collection and RGB Image Transmission. *2017 International Conference on Mechatronics, Electronics and Automotive Engineering (ICMEAE)* (pp. 49-54). IEEE.

Nazzal JM & Natsheh AN 2007. Chaos control using sliding-mode theory. *Chaos, Solitons & Fractals,* 33(2): 695-702.

Njah AN 2010. Tracking control and synchronization of the new hyperchaotic Liu system via backstepping techniques. *Nonlinear Dynamics,* 61(1-2): 1-9.

Okpabi SO, Oke AA, Akinlami JO & Opeifa ST 2017. Backstepping Control and Synchronization of hyperchaotic Lorenz-Stenflo system with application to secure communication. *Far East J. Dynam. Sys.,* 29(1): 1-23.

Onma OS & Akinlami JO 2017. Dynamics, adaptive control and extended synchronization of hyperchaotic system and its application to secure communication. *Int. J. Chaos Control, Modeling and Simulation,* 6(4).

Onma OS, Olusola OI & Njah AN 2016. Control and synchronization of chaotic and hyperchaotic Lorenz systems via extended adaptive control method. *Far East J. Dynam. Sys.,* 28(1): 1.

Onma SO, Adelakun AO, Akinlami JO & Opeifa S 2017. Backstepping control and synchronization of hyperchaotic Lorenz-Stenflo system with application to secure communication. *Far East J. Dynam. Sys.,* 29(1): 1-23.

Park JH & Kwon OM 2003. A novel criterion for delayed feedback control of time-delay chaotic systems. *Chaos, Solitons and Fractals,* 17: 709-716.

Rössler OE 1976. An equation for continuous chaos. *Physics Letters A,* 57(5): 397-398.

Sambas A, Sanjaya WSM & Mamat M 2015. Bidirectional coupling scheme of chaotic systems and its application in secure communication system. *J. Engr. Sci. & Techn. Rev.,* 8(2): 89-95.

Sprott JC 1994. Some simple chaotic flows. *Physical Review E,* 50(2): R647.

Sundarapandian V & Pehlivan I 2012. Analysis, control, synchronization, and circuit design of a novel chaotic system. *Mathematical and Computer Modelling,* 55(7-8): 1904-1915.

Sundarapandian V 2012. Adaptive Control and Szchronization of Sprott-I System with unknown Parameters. *Int. J. Soft Comp., Artif. Intell. and Applic.,* 1(1): 29-41.

Sundarapandian V 2013. Analysis and anti-synchronization of a novel chaotic system via active and adaptive controllers. *J. Engr. Sci. and Techn. Rev.,* 6(4): 45-52.

Tirandaz H & Hajipour A 2017. Adaptive synchronization and anti-synchronization of TSUCS and Lü unified chaotic systems with unknown parameters. *Optik,* 130: 543-549.

Tlelo-Cuautle E & Duarte-Villaseñor MA 2007. Designing Chua's circuit from the behavioral to the transistor level of abstraction. *Applied Mathematics and Computation,* 184(2): 715-720.

Vaidyanathan S & Rhif A 2017. A novel four-leaf chaotic system, its control and synchronisation via integral sliding mode control. *Int. J. Modelling, Identific. and Control,* 28(1): 28-39.

Vaidyanathan S 2012a. Global chaos synchronization of Sprott-L and Sprott-M systems by active control. *Int. J. Control Theory and Comp. Modelling,* 2(4): 21-35.

Vaidyanathan S 2012b. Analysis, control and synchronization of Sprott -K system with unknown parameters. *Int. J. Soft Comp., Maths. and Control,* 1: 1-14.

Vaidyanathan S 2012c. Anti-synchronization of Sprott-L and Sprott-M chaotic systems via adaptive control. *Int. J. Control Theory Appl.,* 5(1): 41-59.

Vaidyanathan S 2015. A novel chemical chaotic reactor system and its output regulation via integral sliding mode control. *Parameters,* 1: 4.

Vaidyanathan S 2017. A conservative hyperchaotic hyperjerk system based on memristive device. In: *Advances in Memristors, Memristive Devices and Systems* (pp. 393-423). Springer, Cham.

Vaidyanathan S, Idowu BA & Azar AT 2015. Backstepping controller design for the global chaos synchronization of Sprott's jerk systems. In: *Chaos Modeling and Control Systems Design* (pp. 39-58). Springer, Cham.

Vincent UE 2008. Chaos synchronization using active control and backstepping control: A comparative analysis. *Nonlinear Analysis: Modelling and Control,* 13(2): 253-261.

Vincent UE, Odunaike RK, Laoye JA & Gbindinninuola AA 2011. Adaptive backstepping control and synchronization of a modified and chaotic Van der Pol-Duffing oscillator. *J. Control Theory and Applic.,* 9(2): 273-277.

Volos CK, Prousalis DA, Vaidyanathan S, Pham VT, Munoz-Pacheco JM & Tlelo-Cuautle E 2016. Kinematic control of a robot by using a non-autonomous chaotic system. In *Advances and Applications in Nonlinear Control Systems* (pp. 1-17). Springer, Cham.

Wang X & Chen G 2012. A chaotic system with only one stable equilibrium. *Communications in Nonlinear Science and Numerical Simulation,* 17(3): 1264-1272.

Wang Z, Sun W, Wei Z & Xi X 2014. Dynamics analysis and robust modified function projective synchronization of Sprott E system with quadratic perturbation. *Kybernetika,* 50(4): 616-631.

Xiao-dong X, Wan-li Y & Su-wen Z 2009. Finite time synchronization of Sprott circuits with uncertain parameters. *2009 Int. Conf. on Advan. Comp. Control* (pp. 693-696). IEEE.

Yılmaz U & Ihsan P 2010. Nonlinear Sprott 94 Case A chaotic equation: Synchronization and masking communication applications. *Computers and Electrical Engineering,* 36: 1093–1100.

Yu F, Li P, Gu K & Yin B 2016. Research progress of multi-scroll chaotic oscillators based on current-mode devices. *Optik,* 127(13): 5486-5490.

Yu-shu M & Jun-hai C 2001. Study for the bifurcation topological structure and the global complicated character of a kind of nonlinear finance system (I). *Applied Mathematicsand Mechanics,* 22(11): 119-128.